

Slicing Pomerons in ultraperipheral collisions using forward neutrons from nuclear breakup

M. Alvioli,^{1,2} V. Guzey,³ and M. Strikman⁴

¹*Consiglio Nazionale delle Ricerche, Istituto di Ricerca per la Protezione Idrogeologica, via Madonna Alta 126, I-06128, Perugia, Italy*

²*Istituto Nazionale di Fisica Nucleare, Sezione di Perugia, via Pascoli 23c, I-06123, Perugia, Italy*

³*University of Jyväskylä, Department of Physics, P.O. Box 35, FI-40014 University of Jyväskylä, Finland and Helsinki Institute of Physics, P.O. Box 64, FI-00014 University of Helsinki, Finland*

⁴*Pennsylvania State University, University Park, PA, 16802, USA*

(Dated: March 1, 2024)

We argue that measurements of forward neutrons from nuclear breakup in inclusive high energy photon-nucleus (γA) scattering provide a novel complementary way to study small- x dynamics of QCD in heavy-ion ultraperipheral collisions (UPCs). Using the leading twist approximation to nuclear shadowing, we calculate the distribution over the number of evaporation neutrons produced in γPb collisions at the LHC. We demonstrate that it allows one to determine the distribution over the number of wounded nucleons (inelastic collisions), which constrains the mechanism of nuclear shadowing of nuclear parton distributions.

PACS numbers:

Keywords: Heavy-ion scattering, ultraperipheral collisions, nuclear shadowing

I. INTRODUCTION AND MOTIVATION

Understanding of the QCD dynamics of hard high energy interactions and the structure of nuclei and nucleons is one of the main directions of theoretical and experimental studies at the Large Hadron Collider (LHC) and the Relativistic Heavy Ion Collider (RHIC). Of particular interest is the limit of very small momentum fractions x , when the linear Dokshitzer-Gribov-Lipatov-Altarelli-Parisi (DGLAP) approximation is expected to break down [1, 2] and a regime close to the black disk limit (BDL) [3] may set in. Its observation is one of the prime objectives of the planned Electron-Ion Collider (EIC) at Brookhaven National Laboratory [4, 5], which will ultimately reach $x \sim 10^{-3}$ for momentum transfers of a few GeV. At the same time, it was pointed out some time ago that ultraperipheral collisions (UPCs) of two ions at the LHC, where a photon emitted by one of the nuclei interacts with the other nucleus, allow one to probe down to $x \sim 10^{-5} - 10^{-4}$, depending on a particular reaction channel and the detector geometry [6, 7].

Electron-nucleus collisions at the EIC and UPCs of heavy ions at the LHC present two options for studying small- x dynamics, which are largely complementary. At the LHC practically all data are collected for one heavy nucleus and one cannot directly access the dependence of cross sections on the virtuality of the probe. At the same time, one can reach very small x , which is provided by a wide rapidity coverage of the LHC detectors and the large invariant photon-nucleus collision energies exceeding by a factor of 100 the design energies at the EIC.

Over the last decade the data taken in the LHC and RHIC kinematics discovered a significant nuclear suppression of coherent J/ψ photoproduction in Pb-Pb and Au-Au UPCs compared to the impulse approximation prediction [8–17]. When interpreted in the leading twist approximation (LTA) [18], it amounts to strong gluon nuclear shadowing [19, 20]:

$$R_A^g(x, Q^2) = \frac{g_A(x, Q^2)}{Ag_N(x, Q^2)} < 1, \quad (1)$$

where $g_A(x, Q^2)$ and $g_N(x, Q^2)$ are the nucleus and nucleon gluon densities, respectively. Typical numbers reported by the LHC experiments [8–16] correspond to

$$\begin{aligned} R_{\text{Pb}}^g(x = 10^{-3}, Q_{\text{eff}}^2 = 3 \text{ GeV}^2) &\approx 0.6, \\ R_{\text{Pb}}^g(x = 10^{-4}, Q_{\text{eff}}^2 = 3 \text{ GeV}^2) &\approx 0.5, \end{aligned} \quad (2)$$

with a similar suppression extending down to $x \sim 10^{-5}$. Here Q_{eff} is the effective resolution scale determined by the charm quark mass. These values of R_{Pb}^g agree very well with the LTA predictions for nuclear shadowing made more than 10 years ago [18]. Note that this interpretation of the J/ψ UPC data is complicated at the next-to-leading order (NLO) of the perturbative expansion in powers of $\log Q^2$ (perturbative QCD) due to large cancellations between the leading-order (LO) and NLO gluon terms, which leaves a numerically important quark contribution [21, 22]. A way to

stabilize the perturbation series and restore the gluon dominance in this process on the proton target was suggested in [23, 24].

Other hard UPC processes considered in the literature are inclusive [6, 25] and diffractive [26] dijet photoproduction, which are still to produce final results [27, 28], timelike Compton scattering [29–31], and heavy quark photoproduction [32–34]. Overall these findings confirm the conclusion of [7] that UPCs provide a very effective tool to access the small- x dynamics of the strong interactions and the nuclear structure in hard, semi-hard and soft regimes.

So far the experimental studies of UPCs have mainly been focusing on coherent and incoherent production of light and heavy vector mesons. In this paper, we would like to outline several possible directions of future UPC studies, which were not discussed in the review [7] due to the lack of experimental confirmations of large nuclear shadowing. We explore for the first time possibilities of testing the small- x nuclear shadowing dynamics by measuring the rates of forward neutron production from nuclear breakup in the zero degree calorimeters (ZDCs) at the LHC. Our numerical studies demonstrate that the number of produced neutrons is correlated with the number of wounded nucleons (inelastic photon-nucleon interactions), which presents a complementary way to study the mechanism of nuclear shadowing of nuclear parton distributions. In particular, this allows one to effectively probe the centrality (impact parameter) dependence of nuclear shadowing by experimentally controlling the number of unitarity cuts of diffractive exchanges (Pomerons), which build up the leading twist nuclear shadowing.

This paper is organized as follows. In Sec. II we briefly summarize expectations based on applications of the Abramovski-Gribov-Kancheli (AGK) theorem to photon-nucleus scattering, model the distribution over the number of wounded nucleons and estimate its average value in the current UPC kinematics. Section III presents our predictions for the distributions over the number of emitted forward neutrons from nuclear breakup in inelastic photon-nucleus scattering and its connection to parameters of the leading twist approximation of nuclear shadowing. Our conclusions and outlook are given Sec. IV.

II. ABRAMOVSKI-GRIBOV-KANCHELI (AGK) CUTTING RULES, NUCLEAR SHADOWING AND THE NUMBER OF WOUNDED NUCLEONS IN γA SCATTERING

It was demonstrated by Abramovski, Gribov and Kancheli in 1973 [35] that different unitary cuts of the diagrams corresponding to multi-Pomeron (color singlet) exchanges result in different multiplicities of produced particles in the central rapidity region and that the absorptive part of the amplitude can be expressed in terms of a small number of cut diagrams, which are related by combinatorial factors; these are the so-called Abramovski-Gribov-Kancheli (AGK) cutting rules or the AGK cancellation. For the interpretation of the AGK rules in QCD and other effective field theories, see Refs. [36–40].

The application of the AGK cutting rules to photon-nucleus scattering allows one to express the nuclear shadowing correction to the total nuclear cross section $\sigma_{\text{tot}}^{\gamma A}$ in terms of the diffractive cross section on individual nucleons [41, 42]. Indeed, the nuclear amplitude can be constructed as a series corresponding to the interactions with $k = 1, 2, \dots, A$ nucleons of the target, which are mediated by Pomeron exchanges. The interaction with one nucleon gives the impulse approximation (IA),

$$\sigma_{\text{tot}}^{\gamma A(\text{IA})} = A \sigma_{\text{tot}}^{\gamma N}, \quad (3)$$

where $\sigma_{\text{tot}}^{\gamma N}$ is the total photon-nucleon cross section. For the interaction with two nucleons, the nuclear cross section is given by a sum of cut two-Reggeon amplitudes corresponding to both Reggeons uncut (σ_0), one cut Reggeon (σ_1), and two cut Reggeons (σ_2),

$$\sigma_{\text{tot}}^{\gamma A(k=2)} = \sigma_0 + \sigma_1 + \sigma_2. \quad (4)$$

Figure 1 shows the diagrams corresponding to the three terms in Eq. (4). The AGK rules relate these cross sections as follows

$$\begin{aligned} \sigma_1 &= -4\sigma_0, \\ \sigma_2 &= 2\sigma_0, \end{aligned} \quad (5)$$

where σ_1 is the absorptive (screening) correction to the IA cross section, and σ_2 corresponds to the inelastic interaction with both nucleons. In Eq. (5), we neglected the small real part of the amplitude for simplicity.

Substituting Eq. (5) in Eq. (4), one finds for the nuclear shadowing correction $\Delta\sigma_{\text{tot}}^{\gamma A}$ in the approximation, where one keeps the interaction with only one and two nucleons,

$$\Delta\sigma_{\text{tot}}^{\gamma A} = \sigma_{\text{tot}}^{\gamma A} - \sigma_{\text{tot}}^{\gamma A(\text{IA})} = \sigma_{\text{tot}}^{\gamma A(k=2)} - A\sigma_{\text{tot}}^{\gamma N} = -\sigma_0. \quad (6)$$

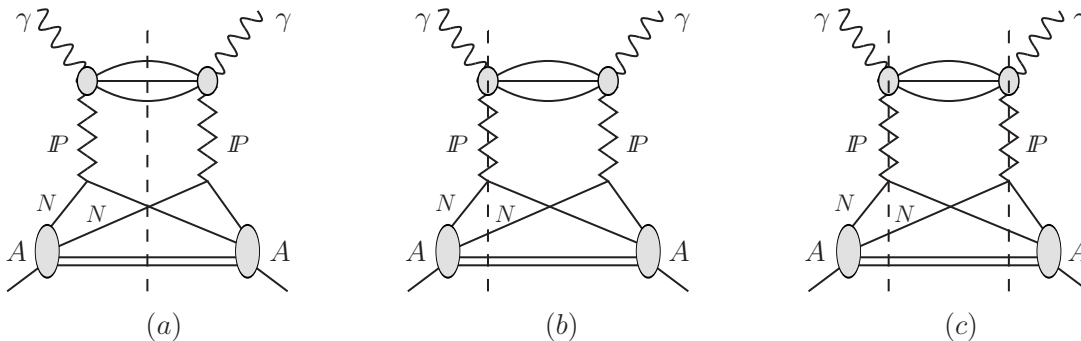


FIG. 1: Unitary cuts of the two-Reggeon forward amplitude, which gives rise to the nuclear shadowing correction due to the interaction with $k = 2$ nucleons of the nuclear target: (a) the diffractive cut with both Reggeons uncut and the cross section σ_0 , (b) one cut Reggeon corresponding to a single multiplicity and the cross section σ_1 , and (c) two cut Reggeons corresponding to a double multiplicity and the cross section σ_2 .

This relation constitutes the foundation of the Gribov model of nuclear shadowing for the total cross section of pion-deuteron scattering, which relates the nuclear shadowing correction to the pion-nucleon diffractive cross section [43]. Note that the AGK rules were derived later and were not explicitly used in [43]. For the generalization of this approach for the calculation of total cross sections of photon scattering on heavier nuclei, see [44–47].

Equation (6) is general and does not require an expansion over twists or the partonic interpretation. However, in lepton-proton deep inelastic scattering (DIS), σ_0 is a leading twist cross section, which by the virtue of the QCD collinear factorization theorem for hard diffraction [48] can be interpreted in terms of diffractive parton distribution functions (PDFs). As a result, it allows one to formulate the leading twist approximation for small- x nuclear PDFs of individual flavors (valence and sea quarks and gluons) [18, 42, 49].

Another important application of the AGK cutting rules involves the total hadron-nucleus inelastic cross section defined as the difference between the total and total elastic (coherent plus incoherent) cross sections, which is obtained using the unitary form of the Glauber theory [50]. Generalizing this result to photon-nucleus scattering by taking into account that the photon takes part in the strong interactions by means of its hadronic fluctuations, the photon-nucleus total inelastic cross section can be presented in the following form [51]

$$\sigma_{\text{inel}}^{\gamma A} = \sum_{\nu=1}^A \sigma_{\nu}, \quad (7)$$

where

$$\sigma_{\nu} = \frac{A!}{(A-\nu)! \nu!} \int d^2 \vec{b} \int d\sigma P_{\gamma}(\sigma) (\sigma_{\text{inel}} T_A(\vec{b}))^{\nu} (1 - \sigma_{\text{inel}} T_A(\vec{b}))^{A-\nu}. \quad (8)$$

In Eq. (8), \vec{b} is the impact parameter (transverse coordinate) of the interacting nucleon, $T_A(\vec{b}) = \int dz \rho_A(\vec{b}, z)$, where $\rho_A(\vec{b}, z)$ is the nuclear density normalized to unity, and $\sigma_{\text{inel}} = 0.85 \sigma$ is the inelastic cross section for the interaction of a hadronic fluctuation of the photon with a target nucleon, which is based on the estimate that the ρ meson-nucleon elastic cross section constitutes approximately 15% of the total one. Unlike the sign-alternating Glauber series for the nuclear total cross section [52], the cross sections σ_{ν} in Eqs. (7) and (8) are positive and represent the physical process, where ν nucleons undergo inelastic scattering, while the remaining $A - \nu$ nucleons provide absorption. In the literature, one uses the term “wounded nucleons” [53] and the notation $\nu = N_{\text{coll}}$.

The distribution $P_{\gamma}(\sigma)$ gives the probability density for hadronic fluctuations of the real photon to interact with nucleons with the cross section σ [51, 54]. While the shape of $P_{\gamma}(\sigma)$ cannot be calculated from the first principles, one can reliably model it using constraints on its first moments and the small- σ and large- σ limits. Indeed, the total photon-proton cross section $\sigma_{\gamma p}(W)$ and the cross section of photon diffractive dissociation on the proton $d\sigma_{\gamma p \rightarrow X_p}(W, t=0)/dt$ constrain the first two moments of $P_{\gamma}(\sigma)$ as follows

$$\begin{aligned} \sigma_{\gamma p}(W) &= \int d\sigma P_{\gamma}(\sigma) \sigma, \\ \frac{d\sigma_{\gamma p}(W, t=0)}{dt} &= \frac{1}{16\pi} \int d\sigma P_{\gamma}(\sigma) \sigma^2, \end{aligned} \quad (9)$$

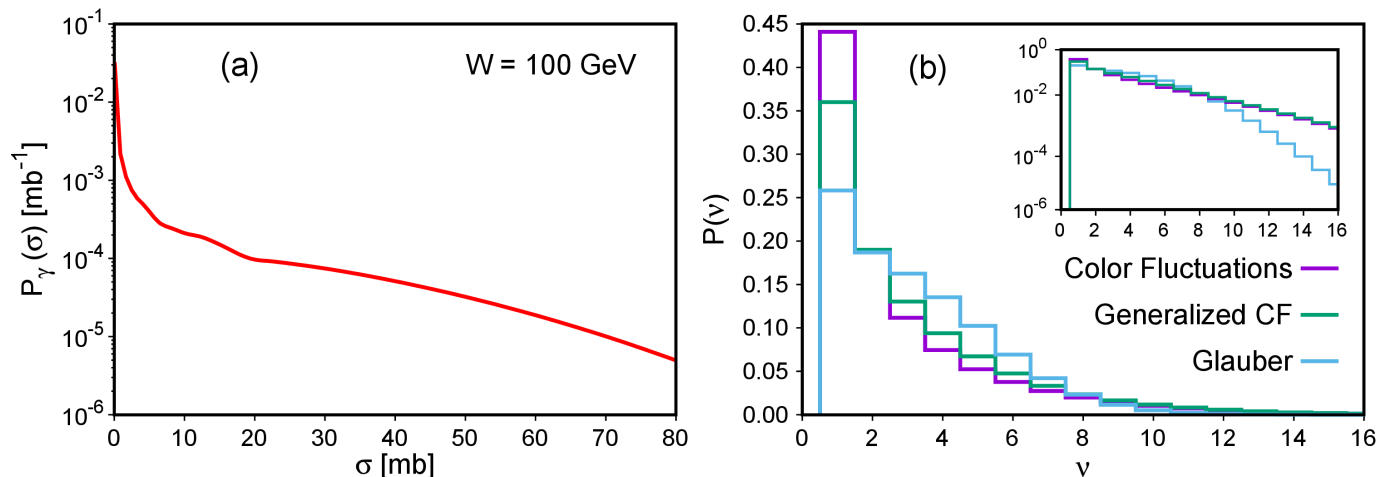


FIG. 2: (a) The $P_\gamma(\sigma)$ probability density for hadronic fluctuations of the real photon to interact with nucleons with the cross section σ at $W = 100$ GeV. (b) The $P(\nu)$ distribution over the number of wounded nucleons (inelastic interactions) ν in inelastic photon-nucleus (Pb) scattering. The three curves correspond to the three models for $P_\gamma(\sigma)$ parametrizing hadronic fluctuations of the real photon, see text for details. The figures are adopted from [51].

where W is the invariant photon-nucleon center-of-mass-energy. Further, in the small- σ limit, one can express $P_\gamma(\sigma)$ in terms of the quark-antiquark component of the photon light-cone wave function and the color dipole cross section, which results in $P_\gamma(\sigma) \propto 1/\sigma$. In the opposite limit of large σ , the photon behaves as a superposition of the ρ , ω and ϕ vector mesons in the spirit of the vector meson dominance model and, hence, $P_\gamma(\sigma)$ can be modeled using hadronic (cross section) fluctuations in ρ mesons, which in turn are related to those for pions. Finally, the small- σ and large- σ regimes can be smoothly interpolated. Note that this matching is achieved best, when the light quark masses m_q are taken to be those of the constituent quarks, $m_q \sim 300$ MeV. For details, see [51, 54].

The left panel of Fig. 2 presents the resulting distribution $P_\gamma(\sigma)$ as a function of σ at $W = 100$ GeV. Its shape and normalization are constrained by the procedure outlined above, the parametrization of $\sigma_{\gamma p}(W)$ [55], and the data on $d\sigma_{\gamma p \rightarrow Xp}(W, t=0)/dt$ [56]. Since the W dependence of $P_\gamma(\sigma)$ is weak, the presented distribution is applicable to a wide range of energies probed in heavy-ion UPCs at the LHC. Note that the distribution $P_\gamma(\sigma)$ parametrizes the so-called resolved photon contribution to photon-induced scattering and does contain the direct photon contribution.

Using Eqs. (7) and (8), one can readily define the $P(\nu)$ probability distribution for the number of wounded nucleons ν in inelastic photon-nucleus scattering as follows [51],

$$P(\nu) = \frac{\sigma_\nu}{\sum_{\nu=1}^A \sigma_\nu}, \quad (10)$$

where σ_ν is given by Eq. (8). To calculate it, we use the Monte Carlo generator for nucleon configurations in complex nuclei [57], which also includes nucleon-nucleon correlations in the nucleus wave function [58, 59], and the Gribov-Glauber model for photon-nucleus scattering, where the hadronic structure of the photon is described by the distribution $P_\gamma(\sigma)$ [51]. The resulting distribution $P(\nu)$ as a function of ν for lead (Pb) is shown by the curve labeled “Color Fluctuations” in the right panel of Fig. 2.

Our modeling of small- σ hadronic fluctuations of the photon is based on the quark-antiquark component of the photon wave function and corresponds to a weak nuclear shadowing in disagreement with the observed strong gluon nuclear shadowing, see Eqs. (1) and (2). To take the latter into account, we model the nuclear suppression of the dipoles with $\sigma \leq \sigma_0 = 20$ mb by the factor of R_A^g , which leads to the modified expression for the distribution $\tilde{P}_\gamma(\sigma)$,

$$\tilde{P}_\gamma(\sigma) = [R_A^g(x, Q_{\text{eff}}^2)\theta(\sigma_0 - \sigma) + \theta(\sigma - \sigma_0)] P_\gamma(\sigma), \quad (11)$$

where $x = Q_{\text{eff}}^2/W^2$ and $P_\gamma(\sigma)$ is shown in Fig. 2 (left panel). The distribution $P(\nu)$ corresponding to σ_ν calculated using $\tilde{P}_\gamma(\sigma)$ is given by the curve “Generalized CF” in the right panel of Fig. 2.

Finally, to test the importance of cross section (color) fluctuations in the real photon, we calculated $P(\nu)$ neglecting these fluctuations and using

$$P_\gamma(\sigma) = \delta(\sigma - 25 \text{ mb}) \quad (12)$$

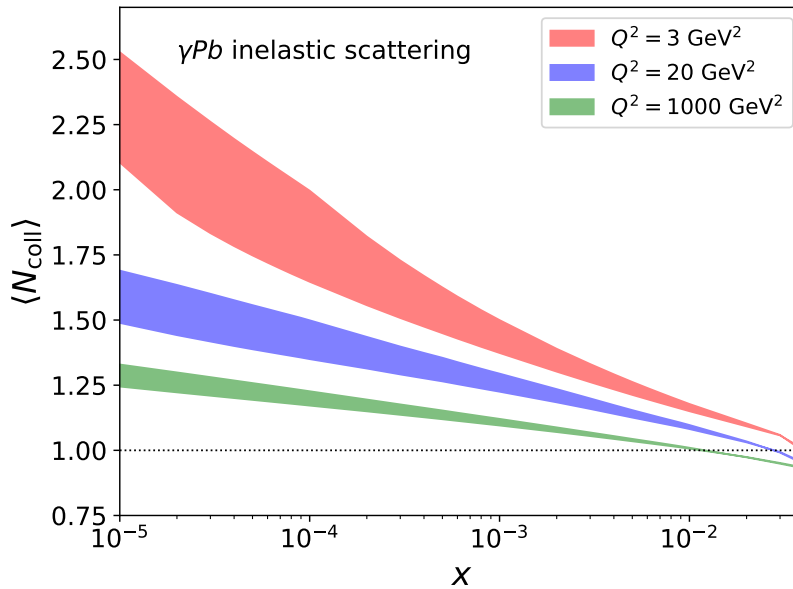


FIG. 3: The LTA predictions for the average number of wounded nucleons $\langle N_{\text{coll}} \rangle$ in inelastic photon-nucleus (Pb) scattering as a function of x at $Q^2 = 3, 20, \text{ and } 1000 \text{ GeV}^2$.

in Eq. (8). The result is given by the curve “Glauber” in Fig. 2. One can see from this figure that color fluctuations significantly increase the distribution $P(\nu)$ at small and especially large σ ; the latter is emphasized in the insert.

In the total inelastic photon-nucleus cross section, the AGK cancellations manifest themselves as the observation that the average number of wounded nucleons $\langle N_{\text{coll}} \rangle$ is inversely proportional to the nuclear shadowing factor. Generalizing the result of [50] for hadron-nucleus scattering to the case of photon-induced scattering, one obtains

$$\langle N_{\text{coll}} \rangle \equiv \sum_{\nu=1}^A P(\nu)\nu = \frac{\sum_{\nu=1}^A \nu \sigma_{\nu}}{\sum_{\nu=1}^A \sigma_{\nu}} = \frac{A \sigma_{\text{inel}}^{\gamma N}}{\sigma_{\text{inel}}^{\gamma A}}, \quad (13)$$

where $\sigma_{\text{inel}}^{\gamma N}$ is the photon-nucleon inelastic cross section. Considering a particular hard process in inelastic photon-nucleus scattering that probes the nuclear gluon distribution, *e.g.*, inclusive charmonium (bottomonium) production $\gamma + A \rightarrow J/\psi(\Upsilon) + X$ or inclusive heavy-quark dijet production $\gamma + A \rightarrow Q\bar{Q} + X$, one obtains using Eq. (13):

$$\langle N_{\text{coll}} \rangle \approx \frac{1}{R_{\text{Pb}}^g(x, Q^2)} \lesssim 2. \quad (14)$$

In this estimate we used the following considerations. In general, the effect of nuclear shadowing for the nuclear inelastic cross section is somewhat larger than that for the total cross section. However, the theoretical uncertainties of the leading twist approximation [18] largely mask the differences and make the shadowing effects approximately equal (within uncertainties) in the two cases. Finally, in the last step, we used the results of Eq. (2).

Figure 3 shows predictions of the leading twist approximation for the average number of wounded nucleons $\langle N_{\text{coll}} \rangle = 1/R_{\text{Pb}}^g(x, Q^2)$ in inelastic photon-nucleus (Pb) scattering as a function of x at $Q^2 = 3, 20, \text{ and } 1000 \text{ GeV}^2$. These values of Q^2 correspond to photoproduction J/ψ , Υ , and high- p_T dijets, respectively. One can see from the figure that in the discussed kinematics, the average number of wounded nucleons is modest and the series in Eq. (13) converges rather rapidly. In particular, we have checked that it is saturated by first six terms with a 5% precision. Note, however, that the convergence slows down in the limit of small x .

Measurements of $\langle N_{\text{coll}} \rangle$ present a new method to study nuclear shadowing in inelastic photon-nucleus scattering. Unlike the observables used so far, the constraint of Eq. (14) indicates that one can perform a “Pomeron surgery” of nuclear shadowing by cutting a small number of Pomeron exchanges controlling the number of inelastic interactions with target nucleons. As a result, it gives an opportunity for an experimental determination of a small number of parameters quantifying nuclear shadowing, which leads to a systematic improvement of its theoretical description. We elaborate on it in the following section.

III. THE DISTRIBUTIONS OVER THE NUMBER OF WOUNDED NUCLEON AND FORWARD NEUTRONS FROM NUCLEAR BREAKUP

While the average number of inelastic interactions $\langle N_{\text{coll}} \rangle$ encodes information on the energy and scale dependence of nuclear shadowing, its dependence on the impact parameter of the collision is averaged over. To obtain a more microscopic description of nuclear shadowing and restore its impact parameter dependence, one needs to determine not only $\langle N_{\text{coll}} \rangle$, but also the entire distribution over the number of wounded nucleons. This can be done using experimental data on the neutron emission resulting from nucleus fragmentation in a given UPC process, *e.g.*, in inclusive quarkonium or dijet photoproduction in heavy-ion UPCs with an additional condition of Xn neutrons in the zero degree calorimeter (ZDC) on the nuclear target side [27, 28].

Very little is known about the dynamics of neutron emission in high energy scattering off heavy nuclei. The ALICE collaboration measured the distribution over the number of collisions $\langle N_{\text{coll}} \rangle$ in proton-nucleus scattering as determined by the energy release (E_T) at central rapidities and the neutron multiplicity as a function of E_T . It was observed that $\langle N_{\text{coll}}(E_T) \rangle$ is linearly proportional to number of evaporation neutrons $\langle M_n(E_T) \rangle$ for the same E_T bins at least up to $\langle N_{\text{coll}} \rangle \sim 10$, for details, see [60]. Note that in our case, $\langle N_{\text{coll}} \rangle$ is much lower, see Eq. (14).

Another important observation made by E665 experiment at Fermilab is that in muon-nucleus deep inelastic scattering (DIS) in coincidence with detection of slow neutrons, $\mu^- + A \rightarrow n + X$, the average neutron multiplicity $\langle M_n \rangle$ for the lead target is [61]

$$\langle M_n \rangle \approx 5. \quad (15)$$

This result has been understood in the framework of cascade models of nuclear DIS [62, 63], where soft neutrons are produced either directly in DIS on a bound nucleon or through statistical decay (de-excitation) of the excited residual nucleus, leading to neutron evaporation¹. The latter mechanism depends strongly on the hadron formation time: to describe the energy spectrum of emitted neutrons, one has to assume that only nucleons and pions with momenta ≤ 1 GeV/c could be involved in final state interactions. A similar conclusion was reached by M. Baker (private communication, 2022) using the BeAGLE Monte Carlo generator [65].

This suggests the following space-time picture of forward neutron production in high energy photon-nucleus scattering. Well before the target, the incoming photon fluctuates into long-lived hadronic components, which pass through the nucleus and interact inelastically with several nucleons. This leads to the creation of holes in the nucleus (particle-hole excitations in terminology of a nuclear shell model), which de-excite and cool the nucleus by evaporating neutrons. It also produces a number of soft particles with the momenta less than 1 GeV/c, which in turn generate more neutrons.

The nucleon fragmentation weakly depends on the incident energy due to Feynman scaling and, hence, it is not significantly affected by the energy conservation constraint, which is important in the case, when one uses hadron multiplicities at central rapidities [66]. In this case, the energy transferred to the rest of the nucleus, which heats the residual nuclear system, is proportional to $\langle N_{\text{coll}} \rangle$. Since the Fermilab data [61] corresponds to the average momentum fraction $\langle x \rangle = 0.015$, where the nuclear shadowing effect is small, one finds that $\langle N_{\text{coll}} \rangle \approx 1$, see Eq. (13). Thus, every inelastic photon-nucleon interaction results on average in 5 forward neutrons.

To test this hypothesis, we perform two numerical studies. First, we consider a simple model, which assumes that the probability density of neutron emission is given by the Poisson distribution and that each hole created in the target nucleus generates independently on average $\langle M_n \rangle$ neutrons. Therefore, the neutron probability distribution for $\nu = \langle N_{\text{coll}} \rangle$ wounded nucleons is

$$P_{\text{Poisson}}(N; \lambda = \nu \langle M_n \rangle) = \frac{(\nu \langle M_n \rangle)^N e^{-\nu \langle M_n \rangle}}{N!}, \quad (16)$$

where N is the number of produced neutrons (neutron multiplicity). The resulting probability density (frequency) for Pb as a function of N is shown in the left panel of Fig. 4. In this estimate, we used $\langle M_n \rangle = 5$, see Eq. (15) and Ref. [61], and $\nu = \langle N_{\text{coll}} \rangle = 1, 2$ or 3 independent neutron emissions (wounded nucleons). One can see from the figure that since the distributions for different ν are peaked at different values of N and do not significantly overlap, the measurement of the forward neutron multiplicity can be used to reliably separate contributions of different numbers of wounded nucleons $\langle N_{\text{coll}} \rangle$. Our analysis also shows that this separation becomes even cleaner with an increase of $\langle M_n \rangle$ (not shown here).

¹ The geometry of the heating is very different from the case of AA collisions, where in each collision a large portion of nucleons in each nucleus interacts and de-excitation of the spectators only occurs close to the interaction surface [64].

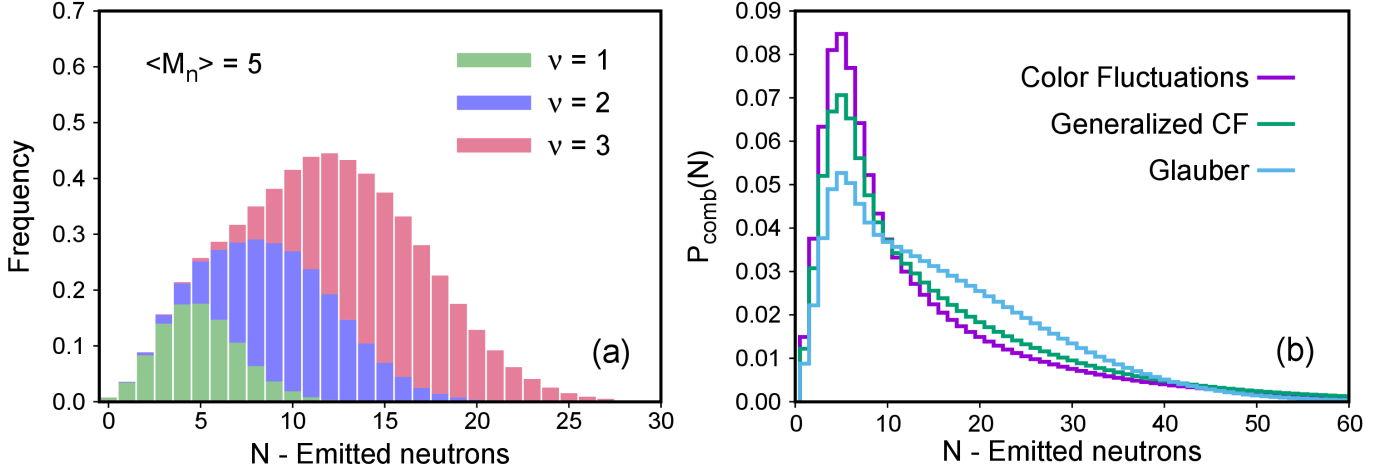


FIG. 4: (a) The probability distribution (frequency) for Pb to produce N forward neutrons assuming their Poisson distribution with $\nu = \langle N_{\text{coll}} \rangle = 1, 2$, and 3 independent emissions (wounded nucleons) and the $\langle M_n \rangle = 5$ average multiplicity for a single inelastic scattering. (b) The probability distribution of forward neutron emission $P_{\text{comb}}(N)$ (17) in the model combining the distribution over the number of wounded nucleons, which is calculated using three models for hadronic fluctuations in the photon (see Fig. 2), with the Poisson distribution of produced neutrons.

In the second study, we combine the distribution over the number of wounded nucleons $P(\nu)$ that we discussed in Sec. II, see Eq. (10) and Fig. 2 (right panel), with the Poisson distribution of produced neutrons, see Eq. (16) and Fig. 4 (left panel). The resulting probability distribution of forward neutrons is given by the following expression,

$$P_{\text{comb}}(N) = \sum_{\nu=1}^A P(\nu) P_{\text{Poisson}}(N; \nu \langle M_n \rangle). \quad (17)$$

The right panel of Fig. 4 presents $P_{\text{comb}}(N)$ as a function of forward neutrons N for $\langle M_n \rangle = 5$. The three curves correspond to the three models for the hadronic (color) fluctuations of the real photon, see the right panel of Fig. 2. One can see from the figure that cross section fluctuations in the real photon noticeably affect the shape of the neutron distribution: its maximum is shifted toward smaller N compared to the ‘‘Glauber’’ result and is also somewhat suppressed by the leading twist shadowing in the ‘‘Generalized CF’’ case.

Our numerical studies suggest that one can examine details of the theoretical description of small- x nuclear shadowing in QCD using the distribution of forward neutrons from nuclear breakup emitted in a given hard UPC process, which is directly correlated with the number of inelastic interactions (wounded nucleons). By studying the dispersion of this distribution, one can single out the individual contributions of $\nu = 1, 2, 3, \dots$ wounded nucleons. In particular, using Eq. (8) in the approximation that the series in Eq. (13) is saturated by first few terms, which corresponds to the limit of small-to-modest nuclear shadowing, one obtains [51, 67]

$$\sigma_2(x, Q^2) \equiv \frac{\langle \sigma_{\text{inel}}^2 \rangle}{\langle \sigma_{\text{inel}} \rangle} = \frac{\langle N_{\text{coll}} - 1 \rangle}{\frac{(A-1)}{2} \int d^2 \vec{b} T_A^2(\vec{b})}, \quad (18)$$

and

$$\sigma_3(x, Q^2) \equiv \frac{\langle \sigma_{\text{inel}}^3 \rangle}{\langle \sigma_{\text{inel}} \rangle} = \frac{\langle \sigma_{\text{inel}}^3 \rangle \langle \sigma_{\text{inel}}^2 \rangle}{\langle \sigma_{\text{inel}} \rangle \langle \sigma_{\text{inel}}^2 \rangle} = \frac{(\langle N_{\text{coll}} - 2 \rangle)(\langle N_{\text{coll}} - 1 \rangle)}{\langle N_{\text{coll}} - 1 \rangle} \frac{\frac{(A-1)}{2} \int d^2 \vec{b} T_A^2(\vec{b})}{\frac{(A-2)(A-1)}{2} \int d^2 \vec{b} T_A^3(\vec{b})}, \quad (19)$$

where $\langle \sigma_{\text{inel}}^n \rangle = \int d\sigma P_\gamma(\sigma) \sigma^n$. The cross sections $\sigma_2(x, Q^2)$ and $\sigma_3(x, Q^2)$ are essential ingredients of the LTA approach [18]. While $\sigma_2(x, Q^2)$ is determined using the HERA data on inclusive diffraction in lepton-proton DIS, $\sigma_3(x, Q^2)$ is model-dependent and leads to theoretical uncertainties of this approach. Thus, an independent determination $\sigma_2(x, Q^2)$ and $\sigma_3(x, Q^2)$ using UPCs with forward neutrons will supply new constraints on these quantities.

Note that to reach a high accuracy in such an analysis, one needs to calibrate the theoretical description against the kinematics, where only one target nucleon is struck, *e.g.*, $\gamma + A \rightarrow 2 \text{ jets} + X$ or quasi-elastic J/ψ production for $x_A \geq 0.01$, where the effect of nuclear shadowing is small, and $\langle N_{\text{coll}} \rangle \approx 1$.

IV. CONCLUSIONS AND OUTLOOK

In this paper, we advertise measurements of forward neutrons from nuclear breakup in inclusive high energy photon-nucleus scattering in heavy-ion UPCs, e.g., charmonium (bottomonium) production $\gamma + A \rightarrow J/\psi(\Upsilon) + X$ or heavy-quark dijet production $\gamma + A \rightarrow Q\bar{Q} + X$, as a novel way to study the QCD dynamics at small x . The key quantity is the number of inelastic photon-nucleon interactions (the number of wounded nucleons): its average value $\langle N_{\text{coll}} \rangle$ is proportional to inverse of the gluon nuclear shadowing and its first moments are sensitive to details of the leading twist mechanism of nuclear shadowing. Our numerical analysis has demonstrated that the number of forward neutrons from nuclear breakup detected in the ZDC on the nuclear target side is rather unambiguously proportional to the number of wounded nucleons, which provides a practical opportunity for novel studies of nuclear shadowing.

On top of providing stringent tests of the dynamics of leading twist shadowing of gluon PDFs, it would be possible to explore effects related to proximity to the black disk limit of the strong interaction. For example, one can study fragmentation of leading hadrons in γA scattering and look for suppression of their multiplicity as a function of Feynman x_F and W as well as for broadening of their transverse momentum distribution [3]. These effects should be more pronounced for central collisions characterized by an enhanced activity in the ZDC. It should be possible to construct from the data an analog of the R_{CP} ratio, which would probe the density dependence of fragmentation. It would also be useful to construct similar quantities for low p_T charm production.

Another interesting application is for multiparton interactions in proton-nucleus (pA) scattering. It was argued in [68] that the single and double scattering can be separated using their dependence on the impact parameter: the former is proportional to A , while the latter $\propto A^{4/3}$. However, since both hard interactions are typically detected in a limited range of rapidities $|y| \leq 3-4$, centrality is difficult to determine from the transverse energy E_T signal because multiparton interactions also contribute to E_T . The use of forward neutrons in ZDCs would alleviate this problem.

One should point out that the neutrons detected in ZDCs can be a promising complementary way to determine centrality of various photon-nucleus and proton-nucleus inelastic collisions expanding the use of ZDCs beyond their current use in vector meson diffractive production and for determining of centrality of the heavy-ion collisions. The main advantage of using forward neutrons rather than the transverse energy E_T for the determination of centrality is a much larger distance in rapidity between the rapidity of the hard process and that of the process used for determination of the centrality.

The methods presented in this paper can be readily generalized to the case of virtual photons and allow one to predict the distribution over the number of forward neutrons in inelastic photon-nucleus scattering at the EIC.

Acknowledgments

The research of V.G. was funded by the Academy of Finland project 330448, the Center of Excellence in Quark Matter of the Academy of Finland (projects 346325 and 346326), and the European Research Council project ERC-2018-ADG-835105 YoctoLHC. The research of M.S. was supported by the US Department of Energy Office of Science, Office of Nuclear Physics under Award No. DE-FG02-93ER40771.

-
- [1] Y. L. Dokshitzer, D. Diakonov and S. I. Troian, Phys. Rept. **58**, 269-395 (1980)
 - [2] L. V. Gribov, E. M. Levin and M. G. Ryskin, Phys. Rept. **100**, 1-150 (1983)
 - [3] L. Frankfurt, V. Guzey, M. McDermott and M. Strikman, Phys. Rev. Lett. **87**, 192301 (2001) [arXiv:hep-ph/0104154 [hep-ph]].
 - [4] A. Accardi, J. L. Albacete, M. Anselmino, N. Armesto, E. C. Aschenauer, A. Bacchetta, D. Boer, W. K. Brooks, T. Burton and N. B. Chang, *et al.* Eur. Phys. J. A **52**, no.9, 268 (2016) [arXiv:1212.1701 [nucl-ex]].
 - [5] R. Abdul Khalek, A. Accardi, J. Adam, D. Adamiak, W. Akers, M. Albaladejo, A. Al-bataineh, M. G. Alexeev, F. Ameli and P. Antonioli, *et al.* Nucl. Phys. A **1026**, 122447 (2022) [arXiv:2103.05419 [physics.ins-det]].
 - [6] M. Strikman, R. Vogt and S. N. White, Phys. Rev. Lett. **96**, 082001 (2006) [arXiv:hep-ph/0508296 [hep-ph]].
 - [7] A. J. Baltz, G. Baur, D. d'Enterria, L. Frankfurt, F. Gelis, V. Guzey, K. Hencken, Y. Kharlov, M. Klasen and S. R. Klein, *et al.* Phys. Rept. **458**, 1-171 (2008)
 - [8] E. Abbas *et al.* [ALICE], Eur. Phys. J. C **73**, no.11, 2617 (2013) [arXiv:1305.1467 [nucl-ex]].
 - [9] B. Abelev *et al.* [ALICE], Phys. Lett. B **718**, 1273-1283 (2013) [arXiv:1209.3715 [nucl-ex]].
 - [10] V. Khachatryan *et al.* [CMS], Phys. Lett. B **772**, 489-511 (2017) [arXiv:1605.06966 [nucl-ex]].
 - [11] S. Acharya *et al.* [ALICE], Eur. Phys. J. C **81**, no.8, 712 (2021) [arXiv:2101.04577 [nucl-ex]].
 - [12] S. Acharya *et al.* [ALICE], Phys. Lett. B **798**, 134926 (2019) [arXiv:1904.06272 [nucl-ex]].
 - [13] R. Aaij *et al.* [LHCb], JHEP **07**, 117 (2022) [arXiv:2107.03223 [hep-ex]].

- [14] R. Aaij *et al.* [LHCb], JHEP **06**, 146 (2023) [arXiv:2206.08221 [hep-ex]].
- [15] A. Tumasyan *et al.* [CMS], Phys. Rev. Lett. **131**, no.26, 262301 (2023) [arXiv:2303.16984 [nucl-ex]].
- [16] S. Acharya *et al.* [ALICE], JHEP **10**, 119 (2023) [arXiv:2305.19060 [nucl-ex]].
- [17] [STAR], [arXiv:2311.13632 [nucl-ex]].
- [18] L. Frankfurt, V. Guzey and M. Strikman, Phys. Rept. **512**, 255-393 (2012) [arXiv:1106.2091 [hep-ph]].
- [19] V. Guzey, E. Kryshen, M. Strikman and M. Zhalov, Phys. Lett. B **726**, 290-295 (2013) [arXiv:1305.1724 [hep-ph]].
- [20] V. Guzey and M. Zhalov, JHEP **10**, 207 (2013) [arXiv:1307.4526 [hep-ph]].
- [21] K. J. Eskola, C. A. Flett, V. Guzey, T. Löytäinen and H. Paukkunen, Phys. Rev. C **106**, no.3, 035202 (2022) [arXiv:2203.11613 [hep-ph]].
- [22] K. J. Eskola, C. A. Flett, V. Guzey, T. Löytäinen and H. Paukkunen, Phys. Rev. C **107**, no.4, 044912 (2023) [arXiv:2210.16048 [hep-ph]].
- [23] S. P. Jones, A. D. Martin, M. G. Ryskin and T. Teubner, J. Phys. G **43**, no.3, 035002 (2016) [arXiv:1507.06942 [hep-ph]].
- [24] S. P. Jones, A. D. Martin, M. G. Ryskin and T. Teubner, Eur. Phys. J. C **76**, no.11, 633 (2016) [arXiv:1610.02272 [hep-ph]].
- [25] V. Guzey and M. Klasen, Phys. Rev. C **99**, no.6, 065202 (2019) [arXiv:1811.10236 [hep-ph]].
- [26] V. Guzey and M. Klasen, JHEP **04**, 158 (2016) [arXiv:1603.06055 [hep-ph]].
- [27] [ATLAS], “Photo-nuclear dijet production in ultra-peripheral Pb+Pb collisions,” ATLAS-CONF-2017-011.
- [28] [ATLAS], “Photo-nuclear jet production in ultra-peripheral Pb+Pb collisions at $\sqrt{s_{NN}} = 5.02$ TeV with the ATLAS detector,” ATLAS-CONF-2022-021.
- [29] B. Pire, L. Szymanowski and J. Wagner, Phys. Rev. D **79**, 014010 (2009) [arXiv:0811.0321 [hep-ph]].
- [30] W. Schafer, G. Slipek and A. Szczurek, Phys. Lett. B **688**, 185-191 (2010) [arXiv:1003.0610 [hep-ph]].
- [31] G. M. Peccini, L. S. Moriggi and M. V. T. Machado, Phys. Rev. D **103**, no.5, 054009 (2021) [arXiv:2101.08338 [hep-ph]].
- [32] S. R. Klein, J. Nystrand and R. Vogt, Phys. Rev. C **66**, 044906 (2002) [arXiv:hep-ph/0206220 [hep-ph]].
- [33] V. P. Goncalves, M. V. T. Machado and A. R. Meneses, Phys. Rev. D **80**, 034021 (2009) [arXiv:0905.2067 [hep-ph]].
- [34] V. P. Goncalves, G. Sampaio dos Santos and C. R. Sena, Nucl. Phys. A **976**, 33-45 (2018) [arXiv:1711.04497 [hep-ph]].
- [35] V. A. Abramovsky, V. N. Gribov and O. V. Kancheli, Yad. Fiz. **18**, 595-616 (1973), Sov. J. Nucl. Phys. **18**, 308-317 (1974).
- [36] D. Treleani, Int. J. Mod. Phys. A **11**, 613-654 (1996)
- [37] J. Jalilian-Marian and Y. V. Kovchegov, Phys. Rev. D **70**, 114017 (2004) [erratum: Phys. Rev. D **71**, 079901 (2005)] [arXiv:hep-ph/0405266 [hep-ph]].
- [38] F. Gelis and R. Venugopalan, Nucl. Phys. A **776**, 135-171 (2006) [arXiv:hep-ph/0601209 [hep-ph]].
- [39] A. Kovner and M. Lublinsky, JHEP **11**, 083 (2006) [arXiv:hep-ph/0609227 [hep-ph]].
- [40] N. N. Nikolaev and W. Schafer, Phys. Rev. D **74**, 074021 (2006) [arXiv:hep-ph/0607307 [hep-ph]].
- [41] L. L. Frankfurt and M. I. Strikman, Phys. Lett. B **382**, 6-12 (1996)
- [42] L. Frankfurt and M. Strikman, Eur. Phys. J. A **5**, 293-306 (1999) [arXiv:hep-ph/9812322 [hep-ph]].
- [43] V. N. Gribov, Sov. Phys. JETP **29**, 483-487 (1969) [Zh. Eksp. Teor. Fiz. **56**, 892-901 (1969)]
- [44] V. N. Gribov, Sov. Phys. JETP **30**, 709-717 (1970) [Zh. Eksp. Teor. Fiz. **57**, 1306-1323 (1969)]
- [45] G. Piller and W. Weise, Phys. Rept. **330**, 1-94 (2000) [arXiv:hep-ph/9908230 [hep-ph]].
- [46] A. Adeluyi and G. Fai, Phys. Rev. C **74**, 054904 (2006) [arXiv:hep-ph/0610214 [hep-ph]].
- [47] A. Adeluyi and T. Nguyen, Phys. Rev. C **75**, 054911 (2007)
- [48] J. C. Collins, Phys. Rev. D **57**, 3051-3056 (1998) [erratum: Phys. Rev. D **61**, 019902 (2000)] [arXiv:hep-ph/9709499 [hep-ph]].
- [49] L. Frankfurt, V. Guzey and M. Strikman, Phys. Rev. D **71**, 054001 (2005) [arXiv:hep-ph/0303022 [hep-ph]].
- [50] L. Bertocchi and D. Treleani, J. Phys. G **3**, 147 (1977)
- [51] M. Alvioli, L. Frankfurt, V. Guzey, M. Strikman and M. Zhalov, Phys. Lett. B **767**, 450-457 (2017) [arXiv:1605.06606 [hep-ph]].
- [52] V. Franco and R. J. Glauber, Phys. Rev. **142**, 1195-1214 (1966)
- [53] A. Bialas, M. Bleszynski and W. Czyz, Nucl. Phys. B **111**, 461-476 (1976)
- [54] L. Frankfurt, V. Guzey, A. Stasto and M. Strikman, Rept. Prog. Phys. **85**, no.12, 126301 (2022) [arXiv:2203.12289 [hep-ph]].
- [55] K. A. Olive *et al.* [Particle Data Group], Chin. Phys. C **38**, 090001 (2014)
- [56] T. J. Chapin, R. L. Cool, K. A. Goulianos, K. A. Jenkins, J. P. Silverman, G. R. Snow, H. Sticker, S. N. White and Y. H. Chou, Phys. Rev. D **31**, 17-30 (1985)
- [57] M. Alvioli, H. J. Drescher and M. Strikman, Phys. Lett. B **680**, 225-230 (2009) [arXiv:0905.2670 [nucl-th]].
- [58] M. Alvioli, C. Ciofi degli Atti, I. Marchino, V. Palli and H. Morita, Phys. Rev. C **78**, 031601 (2008) [arXiv:0807.0873 [nucl-th]].
- [59] M. Alvioli, C. Ciofi degli Atti and H. Morita, Phys. Rev. Lett. **100**, 162503 (2008)
- [60] S. Acharya *et al.* [ALICE], JHEP **08**, 086 (2022) [arXiv:2107.10757 [nucl-ex]].
- [61] M. R. Adams *et al.* [E665], Phys. Rev. Lett. **74**, 5198-5201 (1995) [erratum: Phys. Rev. Lett. **80**, 2020-2021 (1998)]
- [62] M. Strikman, M. G. Tverskoi and M. B. Zhalov, Phys. Lett. B **459**, 37-42 (1999) [arXiv:nucl-th/9806099 [nucl-th]].
- [63] A. B. Larionov and M. Strikman, Phys. Rev. C **101**, no.1, 014617 (2020) [arXiv:1812.08231 [hep-ph]].
- [64] M. Alvioli and M. Strikman, Phys. Rev. C **83**, 044905 (2011) [arXiv:1008.2328 [nucl-th]].
- [65] W. Chang, E. C. Aschenauer, M. D. Baker, A. Jentsch, J. H. Lee, Z. Tu, Z. Yin and L. Zheng, Phys. Rev. D **106**, no.1, 012007 (2022) [arXiv:2204.11998 [physics.comp-ph]].
- [66] G. Aad *et al.* [ATLAS], Eur. Phys. J. C **76**, no.4, 199 (2016) [arXiv:1508.00848 [hep-ex]].
- [67] M. Alvioli, L. Frankfurt, V. Guzey and M. Strikman, Phys. Rev. C **90**, 034914 (2014) [arXiv:1402.2868 [hep-ph]].
- [68] M. Alvioli, M. Azarkin, B. Blok and M. Strikman, Eur. Phys. J. C **79**, no.6, 482 (2019) [arXiv:1901.11266 [hep-ph]].